

Novel hollow fibre membrane reactor for the partial oxidation of methane

Alexandra Kleinert^{a,*}, Armin Feldhoff^a, Thomas Schiestel^b, Jürgen Caro^a

^a *Institute of Physical Chemistry and Electrochemistry, University Hannover, Callinstr. 3-3a, D-30167 Hannover, Germany*

^b *Fraunhofer Institute of Interfacial Engineering and Biotechnology, Nobelstr. 12, D-70569 Stuttgart, Germany*

Available online 21 July 2006

Abstract

In recent years perovskite-type membranes (ABO_3) have been studied intensively as oxygen permeable materials. These perovskite ceramics very often have a disc or tube geometry. In this paper the first data of a membrane reactor for POM with hollow fibres as membrane are reported. The hollow fibres were spun from BCFZ ($\text{Ba}(\text{Co},\text{Fe},\text{Zr})\text{O}_{3-\delta}$) powder. Diluted methane as well as methane with steam were investigated as reaction gases. The spent catalyst was investigated by high-resolution transmission electron microscopy (HR-TEM) after the reaction. Membrane failures were evaluated by field-emission scanning electron microscopy (FE-SEM).

© 2006 Elsevier B.V. All rights reserved.

Keywords: Novel hollow fibre membrane reactor; Perovskite-type membranes; Partial oxidation of methane

1. Introduction

Synthesis gas, a mixture of carbon monoxide and hydrogen, is required for a number of industrial processes, such as methanol or Fischer-Tropsch synthesis. There are several ways of producing syngas from methane, e.g. by the catalytic partial oxidation (POM) (see, e.g. [1], Eq. (1)) or the classical catalytic steam reforming (SR) (see, e.g. [2], Eq. (2)).



Up to now SR is still the main technology although the POM has advantages over the SR. A great advantage of the POM over the SR is the H_2/CO -ratio: for further applications the value of 2 (instead of 3) is optimum. Furthermore, the POM is only slightly exothermal and therefore less cost-intensive than the endothermal SR and can be operated at lower pressures [2]. Furthermore, the POM is kinetically faster than the SR [3].

Of course, neither the POM nor the SR process consists of only one reaction. In fact, both processes form a complex

reaction network. The product of the SR is a gas mixture of CO , CO_2 , H_2 and H_2O . Via dry-reforming, water–gas shift, methane decomposition and Boudouard reaction, synthesis gas is formed as the main product [4]. A typical catalyst for SR is nickel supported on modified and promoted Al_2O_3 [2]. For the catalytic POM two different mechanisms depending on the catalyst used are suggested. Hickmann and Schmidt [3] found hints for methane pyrolysis followed by an oxidation of the carbon over Pt and Rh catalysts. For a Ni-based catalyst Dissanayake et al. [5] proposed a mechanism which includes methane decomposition as the initial step.

A disadvantage of the POM is the cost-intensive air fractionation, which generates the most significant cost in this process. Nitrogen cannot be tolerated in the reaction zone because it would convert to NO_x . This problem led to the idea of the combination of the POM with oxygen conducting materials in a membrane reactor. As oxygen conducting materials, perovskites, perovskite-related structures and stabilized zirconia were investigated by different groups [6–11]. Owing to their high electronic and ionic conductivity at relatively low temperature, which lead to high oxygen fluxes through the membrane, perovskites mostly were investigated for membrane reactors.

On the one hand, thin membranes with a high surface/volume-ratio are required for high oxygen fluxes. The hollow

* Corresponding author. Tel.: +49 511 762 2942; fax: +49 511 762 19121.
E-mail address: alexandrakleinert@gmx.net (A. Kleinert).

fibre geometry provides high surface/volume-ratio. A membrane reactor equipped with 0.85 mm hollow fibres shows c. 4 m² membrane area per m³. On the other hand, it is important to select a suitable material, high oxygen conductivity and high thermal and chemical stability at temperatures $T > 800$ °C in reducing atmospheres are required. Under reducing conditions (e.g. synthesis gas) on the one side of the membrane and air on the other side, the gradient of the oxygen potential over the membrane becomes high. This high gradient is of course the driving force for the transport of the oxygen ions and the electrons, but it is also the driving force for transport of the cations. This may lead to a kinetic decomposition [12], and thus to a failure of the membrane.

Under syngas conditions, examples of unstable perovskite compositions are $\text{Sr}(\text{Fe}_{0.2}\text{Co}_{0.8})\text{O}_{3-\delta}$ [13] and $(\text{La}_{0.2}\text{Sr}_{0.8})(\text{Fe}_{0.2}\text{Co}_{0.8})\text{O}_{3-\delta}$ in tubular geometry [14]. This instability is due to the mentioned kinetic lattice decomposition. Jin et al. [15] found $(\text{La}_{0.2}\text{Sr}_{0.8})(\text{Fe}_{0.2}\text{Co}_{0.8})\text{O}_{3-\delta}$ in disc geometry to be stable. They explained this result with a continuous transport of oxygen through the membrane. They also found the $(\text{La}_{0.6}\text{Sr}_{0.4})(\text{Co}_{0.2}\text{Fe}_{0.8})\text{O}_{3-\delta}$ material to be stable under POM conditions for 3–7 h.

Some groups reported the intrinsic catalytic behaviour of perovskites in the CH_4 -conversion [10,14]. In literature [10], it was found that some materials show catalytic activity towards oxidation and some towards oxidative coupling to higher hydrocarbons. Nevertheless in both cases the conversion of methane was quite low ($\leq 3.35\%$). Balachandran et al. [14] showed that over the non-perovskite material $\text{SrCo}_{0.5}\text{FeO}_{3-\delta}$ methane was converted up to 35% with a selectivity of around 90% to CO_2 . Owing to the low conversion rate and the low CO selectivity of the perovskite itself, a conventional Ni-based reforming catalyst was used in this work, so that the low catalytic activity of the used membrane can be neglected.

Jin et al. [15] investigated a tubular membrane reactor made from $\text{La}_{0.6}\text{Sr}_{0.4}\text{Co}_{0.2}\text{Fe}_{0.8}\text{O}_{3-\delta}$ packed with $\text{NiO}/\text{Al}_2\text{O}_3$ catalyst. In this reactor the conversion of methane was nearly 100% but the CO selectivity was lower than 70%. They explained this low selectivity with the oxidation state of the catalyst: the more reactive form for the conversion to synthesis gas is Ni^0 , which is formed by the reducing atmosphere of CO and H_2 . First, some synthesis gas has to be formed, then the catalyst will undergo the reduction to metallic Ni. In a co-feed reactor this process can happen very easily, because the oxygen which is fed into the reactor will be consumed, so the oxygen partial pressure will decrease very sharply. In contrast, in a membrane reactor the oxygen partial pressure is low but nearly constant over the whole length of the membrane. Therefore the authors reduced the catalyst with hydrogen before starting the reaction. The result was a sharp increase in the CO selectivity ($S_{\text{CO}} = 100\%$) but a slight decrease in the methane conversion ($X_{\text{CH}_4} = 84\%$).

Shao et al. [16] studied $(\text{Ba}_{0.5}\text{Sr}_{0.5})(\text{Co}_{0.8}\text{Fe}_{0.2})\text{O}_{3-\delta}$ in a disc shape with NiAlO_4 as catalyst. After approx. 1 h the methane conversion was below 10% with a CO selectivity of only 20%. After 21 h the methane conversion increases up to 98% and the CO selectivity up to 93%. The reason for this increase in the conversion is also the oxidation state of the Ni-based catalyst.

As mentioned above, Balachandran et al. [14] studied the non-perovskite phase $\text{SrCo}_{0.5}\text{FeO}_x$ in a tubular membrane reactor with a Rh-based catalyst. They reached a methane conversion of about 98% with a CO selectivity of 90%. This set-up was only stable for 70 h.

In this paper a perovskite $\text{Ba}(\text{Co,Fe,Zr})\text{O}_{3-\delta}$ (BCFZ) is used, which represents a very suitable material. It is stable and has a good oxygen conductivity [17,18]. It is a good compromise between high conductivity and sufficient stability. This perovskite was spun to hollow fibres to reach a high surface/volume-ratio for the use in a membrane reactor for the POM.

2. Experimental

2.1. Preparation of the hollow fibres

The hollow fibres were prepared by phase inversion spinning at the Fraunhofer Institute for Interfacial Engineering and Biotechnology [19]. The perovskite powder was mixed with a solution of polysulfone (PSU) in 1-methyl-2-pyrrolidone (NMP) (solid content 50–60 wt.%) and was ball milled for 24 h to obtain a homogeneous slurry. This slurry was spun through a spinneret. The cutted green fibres (length 0.5 m, inner diameter 1 mm) were sintered at 1320 °C for 5 h. After this sintering process the hollow fibres had a length of 30 cm, an outer diameter of 800–900 μm and a wall thickness of about 160 μm (Fig. 1).

2.2. Studies in the hollow fibre membrane reactor

The reaction was carried out in the membrane reactor shown in Fig. 2. The reactor consisted of a ceramic tube with an outer diameter of 6 mm, an inner diameter of 4 mm and a length of 24 cm. The Ni-based catalyst with a particle size of 160–320 μm was placed outside the hollow fibre. The mass of the catalyst was varied from 700 to 1000 mg. The temperature was measured with a thermocouple outside the reactor. The

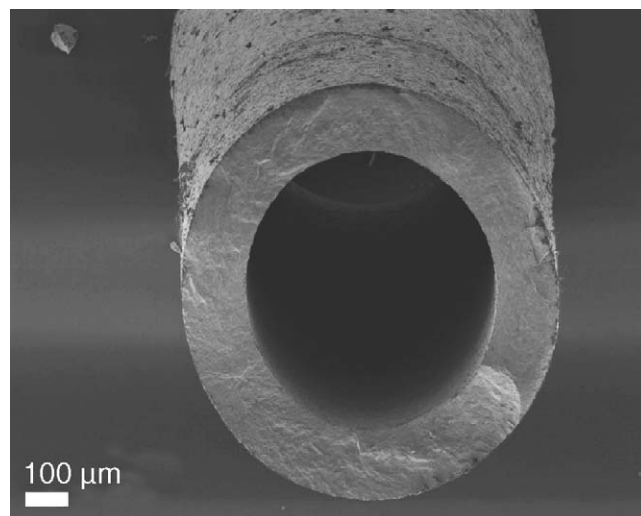


Fig. 1. SEM image of the cross section of BCFZ hollow fibre. The outer diameter is 800–900 μm and the wall thickness 160 μm .

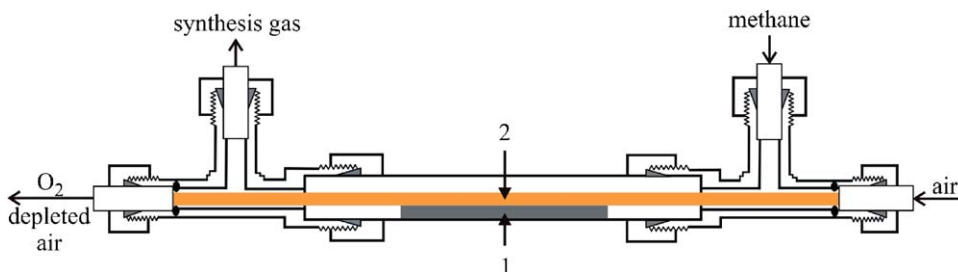


Fig. 2. Membrane reactor for the catalytic partial oxidation of methane; air on the core side; feed on the shell side; 1: catalyst bed, 2: perovskite membrane.

membrane reactor was heated up to 850 and 865 °C, respectively, without any gas stream. When the temperature was achieved, air (purity 99.9995%) and the feed were fed into the reactor, air on the core side and feed on the shell side (co-current operation).

The feed consisted of methane, helium, neon (methane purity 99.5%, helium purity 99.996%, neon purity 99.995%) and in some cases steam. Neon was needed as an inert internal standard to consider dilution effects in the reaction gas mixture. The gas flows were controlled by mass flow controllers (Mättig GmbH). Steam was generated from double distilled water in a controlled evaporator unit (CEM, Mättig GmbH) and mixed with helium in a defined ratio. The feed flow rate and the methane content were varied independently of each other. For the measurements without steam at $T = 865$ °C the feed flow rate was 25, 30, 35, 50 and 65 mL/min and the content of methane 27, 33, 40, 50 and 60 vol.%. The air flow rate was kept constant at 75 mL/min. For the a feed flow rate of 50 and 65 mL/min with a methane content of 40 and 50 vol.% the air flow rate was varied (60 and 90 mL/min) additionally.

For the measurement with steam at $T = 850$ °C the air flow rate was 150 mL/min and the H_2O/CH_4 -ratio 0.5, 1.0 and 2.0, respectively. The total feed flow varied from 40, 50, 60, 70 to 80 mL/min.

The educts as well as the products were analysed for by gas chromatography (HP 6890N), which was connected on-line to the reactor. The conversion with respect to the methane was calculated as:

$$X_{CH_4} = \frac{F_{CO} + F_{CO_2}}{F_{CO} + F_{CO_2} + F_{CH_4, out}} \quad (3)$$

with F_i = flux of component i .

The selectivity of carbon monoxide formation was calculated as:

$$S_{CO} = \frac{F_{CO}}{F_{CO} + F_{CO_2}} \quad (4)$$

The selectivity of carbon dioxide formation was determined $S_{CO_2} = 1 - S_{CO}$.

The carbon balance in the experiments performed was (100 ± 10)%.

The oxygen permeation flux was calculated as:

$$J_{O_2} = \frac{1}{2}F_{CO} + F_{CO_2} + \frac{1}{2}F_{H_2O} \quad (5)$$

2.3. Electron microscopy investigations

Membrane failure was investigated in a field-emission scanning electron microscope (FE-SEM) of the type Jeol JSM-6700F that was equipped with a light-element energy-dispersive X-ray spectrometer (EDXS) of the type Oxford Instruments INCA 300. Samples of the catalyst used in the POM were crushed in a mortar, dispersed in ethanol and fixed on copper supported holey carbon films for transmission electron microscopy (TEM). Microstructural investigations where performed in bright field (BF), dark-field (DF) and high-resolution (HR-TEM) mode at 200 kV in a field-emission instrument of the type Jeol JEM-2100F with an ultra high resolution pole piece that provides a point resolution better than 0.19 nm.

3. Results and discussion

3.1. POM reaction with methane as feed

The hollow fibres used in the POM membrane reactor were stable up to 76 h. As it will be shown, the membrane failure is a break of the hollow fibre due to mechanical deformation caused by coke deposition on the Ni-based catalyst.

As expected, the comparison between the measurements at 35 and 50 mL/min feed flow rate in Fig. 3 shows that a lower feed flow, i.e. a higher contact time and lower gas hourly space velocity (GHSV), respectively, led to higher CH_4 -conversions. For both feed flow rates the CO -selectivity increased with increasing CH_4 -content in the feed. This is due to the fact, that a higher CH_4 -content at constant feed flow means a higher partial

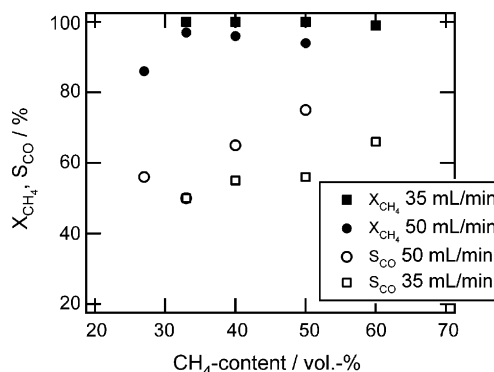


Fig. 3. CH_4 -conversion (X_{CH_4}) and CO -selectivity (S_{CO}) vs. CH_4 -content at $T = 865$ °C; core side: 75 mL/min air; shell side: methane diluted with helium.

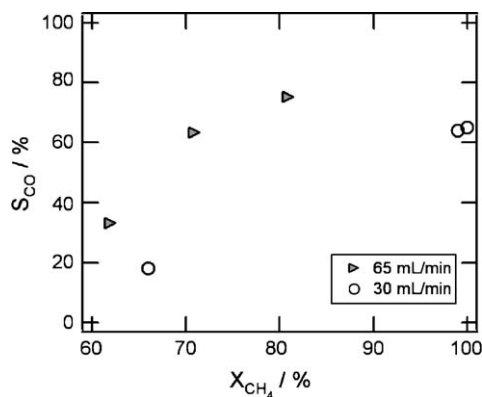


Fig. 4. CO-selectivity (S_{CO}) vs. CH_4 -conversion (X_{CH_4}) with constant feed flow rate at $T = 865^\circ C$; core side: 75 mL/min air; shell side: methane diluted with helium.

pressure of CH_4 . The oxygen partial pressure also increased because the increasing CH_4 -partial pressure leads to a higher consumption of oxygen and thus to a higher O-gradient as driving force over the membrane. But the increase in the CH_4 -concentration is higher than the increase in the oxygen partial pressure [20,21]. So the CH_4/O_2 -ratio increased and, therefore, the reaction to CO is favoured.

While the conversion increased for low feed flows, the CO-selectivity decreased (see Fig. 3). A reason can be the higher contact time, but it can be also an effect of the different conversion degrees. As the difference in the CH_4 -conversion is quite small, the first reason is the more probable one. For further considerations, Fig. 4 shows the CO-selectivity versus the CH_4 -conversions for two different feed flow rates (30, 65 mL/min). A higher feed flow led to higher CO-selectivities for equal CH_4 -conversions. A higher CH_4 -conversion at constant feed flow rate leads to higher CO-selectivities.

The influence of the air flow rate can be seen from Fig. 5. For a CH_4 -content of 40 vol.% the CO-selectivity increased with increasing air flow rate. However, since the CO-selectivities were determined at different CH_4 -conversions ($X_{CH_4} \approx 81\%$ for 60 mL/min air and $X_{CH_4} \approx 100\%$ for 75 and 90 mL/min air)

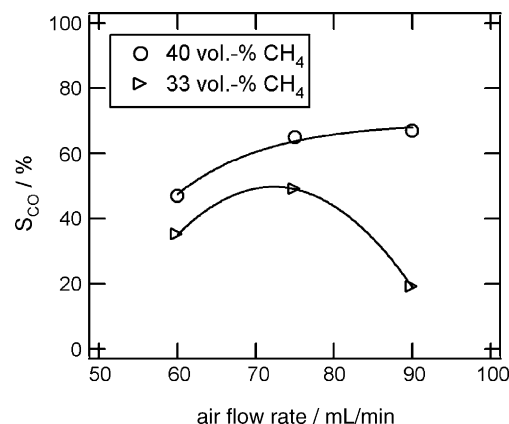


Fig. 5. CO-selectivity (S_{CO}) vs. air flow rate (core side) at $T = 865^\circ C$; shell side: 50 mL/min methane diluted with helium.

these data cannot be compared and a clear trend cannot be seen from these data. For a CH_4 -content of 33 vol.% the CO-selectivity goes through a maximum for an air flow rate of 75 mL/min (conversion for every data point around 100%). A decrease with increasing air flow rate was expected because of an decrease in the CH_4/O_2 -ratio by increasing the oxygen partial pressure. One possibility for this low selectivity for a low air flow rate might be, that not enough oxygen was permeated through the membrane so that the CH_4 decomposed and formed coke. The coke formation and deposition on the catalyst and the fibre was studied, after the hollow fibre was broken. The fibres were investigated by FE-SEM and the catalyst by TEM as shown in Section 3.2.

The highest oxygen permeation flux through the perovskite membrane under study was achieved for a feed flow rate of 35 mL/min with a CH_4 -content of 40 vol.% and an air flow rate of 90 mL/min. It amounts 14.3 mL/min cm^2 .

In comparison with the literature, in this study lower CO-selectivities were found: 80% CO-selectivity at 94% CH_4 -conversion and 83% CO-selectivity at 82% CH_4 -conversion (not shown in the Figs.), respectively. These lower selectivities are due to the higher dilution of the methane, e.g. [15] $CH_4:He = 1:14.5$, or to a different kind of catalyst [13].

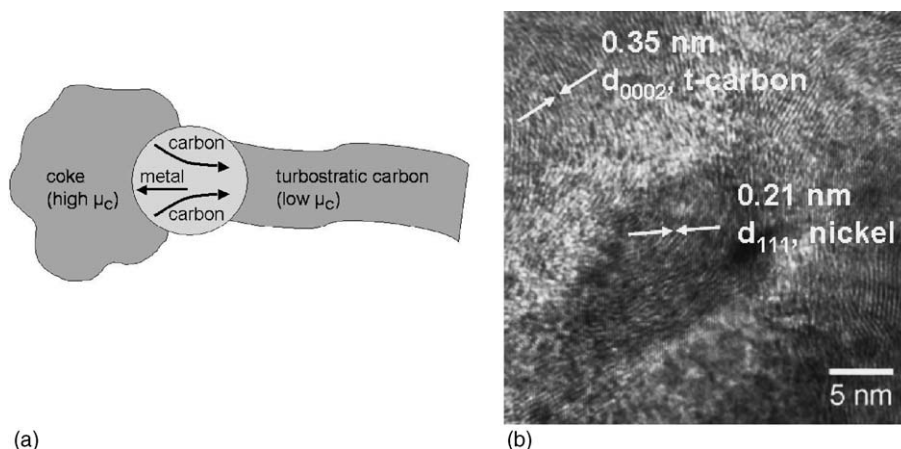


Fig. 6. (a) Scheme of catalytic graphitization of coke, (b) HR-TEM of nickel and lamellar carbon.

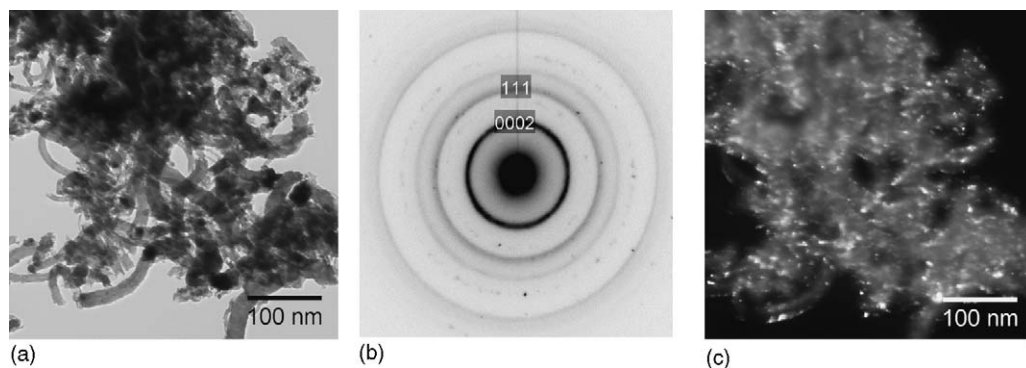


Fig. 7. TEM micrographs of transformed coke intermixed with nickel: (a) bright field; (b) selected area diffraction; (c) dark field.

3.2. Electron microscopy investigations

Coke is formed by several reactions from the mentioned complex network, e.g. the Boudouard reaction and the CH_4 -decomposition. Once coke is present, it is isothermally transformed to lamellae of turbostratic carbon by the migration of nickel particles. This phenomenon is known as catalytic graphitization, the thermodynamics of which is described to some extent in literature [22–25]. During the catalytic graphitization the relatively disordered carbon (high chemical potential of carbon, μ_c) is dissolved by the metal particles, diffuses through the metal particle and precipitate turbostratic carbon lamellae of lower chemical potential (Fig. 6a). The difference in the value of the free enthalpies ΔG is in the order of 30–50 kJ per mole carbon at $T = 850^\circ\text{C}$ [23]. In the high-resolution micrograph in Fig. 6b, a nickel particle with the (1 1 1) lattice fringes of 0.21 nm shows up as well as adherent carbon lamellae with d_{0002} fringes of 0.35 nm. Owing to the turbostratic structure [26] the plane spacing is slightly larger than what would be expected for well-ordered graphite. During the course of the operation, nickel particles migrate through the whole free space and leave lamellar carbon behind them. A ball of lamellae with thicknesses in the range of 10–20 nm is shown in Fig. 7 in bright-field as well as in dark-field contrast. The DF micrograph of Fig. 7c shows the turbostratic carbon with light grey contrast and some nickel particles that are in preferential

diffraction condition as light spots. The evolution of carbon lamellae may cause a constipation of the sweep pathway and finally a breakdown of the membrane reactor. In conclusion, this regime of operation should be strictly avoided. That can be achieved reliably by keeping the steam content at a high level.

For evaluation of whether the breakdown of the membrane is due to a chemical instability (decomposition of the material) or to a mechanical instability because of the formation of coke, the cross-sections of the fibre were investigated by EDXS. It was found that the elements are distributed evenly (results not shown here). There is no enrichment of special elements on the core and on the shell side, respectively. The XRD of the grinded spent hollow fibre showed the unchanged perovskite structure. That is to say the break down of the fibre is only due to the coke formation. To avoid this coke formation, steam was added to methane as reaction gas.

3.3. POM reaction with methane and steam as feed

The POM reaction was investigated with methane and steam as reaction gases. The hollow fibres were stable for up to 65 h. As it will be shown, the membrane failure was due to the formation of BaCO_3 .

The CH_4 -conversions increased from around 84% within 20 min after the gases were fed into the reactor up to c. 100% after 3 h (see Fig. 8). Simultaneously the CO -selectivity

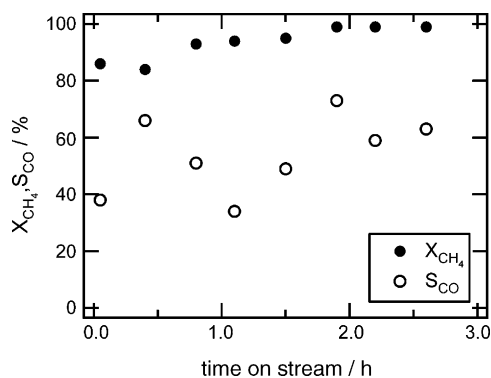


Fig. 8. Time dependence of the CH_4 -conversion (X_{CH_4}) and the CO -selectivity (S_{CO}), respectively, $T = 850^\circ\text{C}$, 60 mL/min feed flow rate, 30 vol.% CH_4 -content.

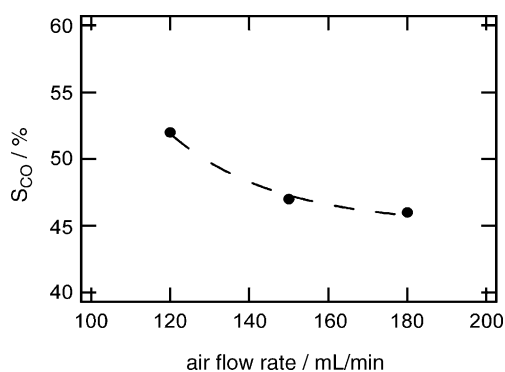


Fig. 9. CO -selectivity (S_{CO}) vs. air flow rate (core side); $T = 850^\circ\text{C}$, 40 mL/min feed flow rate, 30 vol.% CH_4 -content, $X_{\text{CH}_4} = 100\%$.

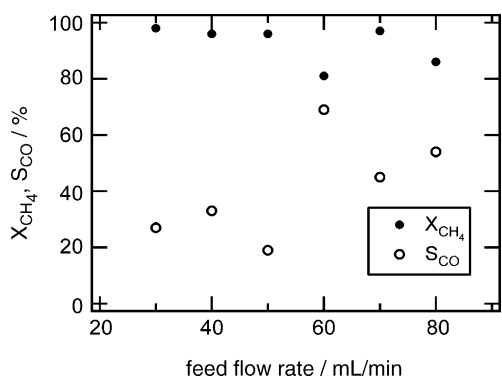


Fig. 10. CH_4 -conversion (X_{CH_4}) and CO-selectivity (S_{CO}), respectively vs. feed flow rate (shell side); $T = 850\text{ }^\circ\text{C}$, 30 vol.% CH_4 -content, $\text{H}_2\text{O}/\text{CH}_4 = 1.0$.

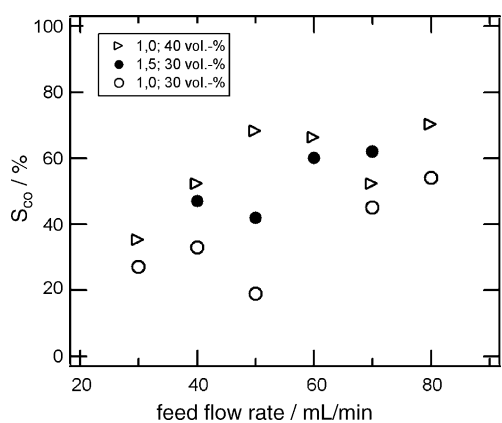


Fig. 11. CO-selectivity (S_{CO}) vs. feed flow rate (shell side) at different $\text{H}_2\text{O}/\text{CH}_4$ -ratios and CH_4 -contents; $T = 850\text{ }^\circ\text{C}$.

fluctuated, but the trend is an increase with reaction time: from 40 to 60%. This result is in accordance with literature data [15]. As mentioned above, a possible explanation for this initial low selectivity is that in a membrane reactor the NiO-based catalyst cannot be reduced so easily as in a co-feed reactor. After the 3 h of reaction shown in Fig. 8 the hollow fibre was still stable and the new reaction conditions were established.

The dependence of the CO-selectivity from the air flow rate can be seen in Fig. 9. With an increase in the air flow rate (from 120, 150 up to 180 mL/min) the CO-selectivity decreased

Table 1

CH_4 -conversion for different feed flow rates and different $\text{H}_2\text{O}/\text{CH}_4$ -ratios; $T = 850\text{ }^\circ\text{C}$, 30 vol.% CH_4

	X_{CH_4} (%) (feed flow rate 40 mL/min)	X_{CH_4} (%) (feed flow rate 50 mL/min)	X_{CH_4} (%) (feed flow rate 70 mL/min)
$\text{H}_2\text{O}/\text{CH}_4 = 1.0$	97	96	97
$\text{H}_2\text{O}/\text{CH}_4 = 1.5$	100	98	100

slightly from 52 to 46%. This increase is due to a slight increase in the oxygen permeation flux: the higher the air flow rate, the higher the oxygen flux [17]. For a higher air flow rate the oxygen partial pressure in the reaction mixture is higher (before the consumption) and, therefore, the total oxidation of methane to CO_2 is preferred.

From Fig. 10 it can be seen, that the CO-selectivity increased with increasing feed flow rate, at constant CH_4 -content. For a feed flow rate of 60 mL/min a high selectivity of CO (around 70%) can be achieved. This is due to the fact, that the CH_4 -conversions decreased for this condition and selectivities at different conversion cannot be compared. In contrast to the measurements without steam, in these measurements there is no clear trend in the CO-selectivity for increasing CH_4 -conversion and will be therefore not discussed. The increase in the CO-selectivity (at nearly constant conversion) with increasing feed flow rate is a result of the lower contact time: a low contact time favours partial oxidation, while a high contact time favours the total oxidation.

In the SR-process high $\text{H}_2\text{O}/\text{CH}_4$ -ratios reduce the CH_4 -conversions because of a catalyst inhibition [1]. In the POM membrane reactor with addition of steam in the feed gas, this influence cannot be proved for ratios of 1.0 and 1.5 (see Table 1). For both conditions the conversion is around 100%. From the literature it is known that a high steam content favours the production of carbon dioxide [27]. This means, a high steam content leads to a decreasing CO-selectivity and, hence, to a possible failure of the membrane because of a reaction between the Ba^{2+} -ions and CO_2 to BaCO_3 . Dosing of steam is necessary to avoid coke formation. It is important, therefore, to evaluate the perfect $\text{H}_2\text{O}/\text{CH}_4$ -ratio. The influence of the $\text{H}_2\text{O}/\text{CH}_4$ -ratio on the CO-selectivity is shown in Fig. 11 for the ratios of 1.0

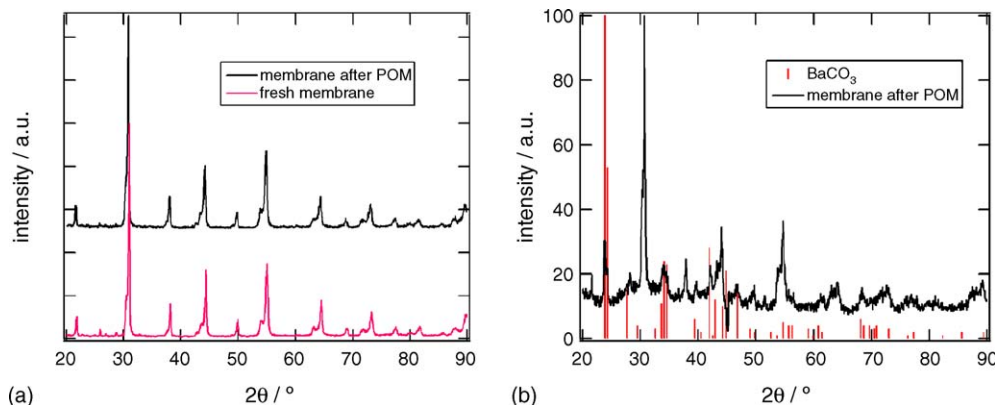


Fig. 12. (a) XRD pattern of the fresh hollow fibre; (b) XRD pattern of the hollow fibre at the exit of the reactor compared with pattern of BaCO_3 .

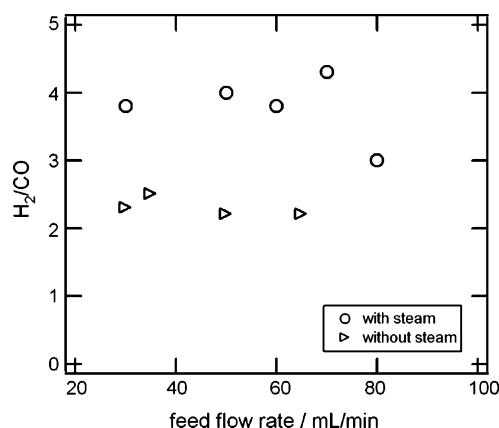


Fig. 13. Comparison of the H_2/CO -ratio from the measurements without steam and with steam in the reaction gas for different feed flow rates; $T = 850^\circ C$, 40 vol.% CH_4 , $H_2O/CH_4 = 1.0$.

and 1.5. As discussed before, the CO-selectivity increased with increasing flow rate. Contrary to the literature [27] the CO-selectivity increased when the H_2O/CH_4 -ratio was increased from 1.0 to 1.5. The influence of the CH_4 -content in the feed on the CO-selectivity is shown as well in Fig. 11. As expected the CO-selectivity (at constant CH_4 -conversion) increased for a higher methane content. For the measurements with an H_2O/CH_4 -ratio of 1.0 as of 1.5 there is no coke formation on the catalyst. In Fig. 12 the XRD patterns of the hollow fibre before the reaction (a) and after the reaction (b) are shown. For the measurements of the fibre after the reaction samples from the middle of the reactor (hot zone) as well as from the exit (colder zone) were taken. Between the fresh fibre and the sample from the hot zone no differences can be noticed in the XRD. But for the sample from the colder exit of the reactor the formation of $BaCO_3$ can be observed. $BaCO_3$ is formed because of a relatively high CO_2 -amount in the gas. The lower temperature at the exit of the reactor favours the formation of the carbonate.

Fig. 13 shows the different H_2/CO -ratios as a function of the feed flow rate for the measurements with and without steam in the feed gases. There is nearly no influence of the feed flow rate on the H_2/CO -ratio. But it can be seen, that the H_2/CO -ratio is smaller for the experiments without steam. The value is around 2 as expected from the direct partial oxidation. For the measurements with steam, the value is between 3.5 and 4.0. One possibility for this higher value is that with steam in the reaction gases the whole network of reactions from the SR can take place. In Table 2 it can be seen, that for the higher H_2O/CH_4 -ratio of 1.5 the H_2/CO -ratio is larger than for the ratio of

Table 2
 H_2/CO -ratio for different H_2O/CH_4 -ratios and feed flow rates; $T = 850^\circ C$, 30 vol.% CH_4

	H_2/CO (feed flow rate 40 mL/min)	H_2/CO (feed flow rate 50 mL/min)	H_2/CO (feed flow rate 60 mL/min)
$H_2O/CH_4 = 1.0$	2.9	2.9	3.2
$H_2O/CH_4 = 1.5$	3.3	4.3	3.8

1.0. For an increase in the feed flow rate no trend can be seen in the H_2/CO -ratio.

4. Conclusion

The POM to form synthesis gas was studied in a novel hollow fibre membrane reactor. The POM was studied for different feed and air flow rates and different CH_4 -contents in the feed. The BCFZ hollow fibres showed a good chemical stability under POM and a lower stability under POM plus steam conditions.

For a CH_4 -conversion of 82% a CO-selectivity of 83% was found. The oxygen permeation flux was of the order of 5–7 mL/min cm^2 at $T = 865^\circ C$.

To avoid coke formation additional measurements with steam in the feed were performed. The highest CO-selectivity (71%) at a CH_4 -conversion of 100% were achieved at a feed flow rate of 80 mL/min, a CH_4 -content of 40 vol.%, a H_2O/CH_4 -ratio of 1.0, and an air flow rate of 150 mL/min. As mentioned above the CO-selectivity increases with an increase in the H_2O -content from the H_2O/CH_4 -ratio of 1.0–1.5. It is possible that the selectivity from 70% can be increased by increasing the H_2O/CH_4 -ratio. An increase in the selectivity should improve the stability of the fibre because the formation of $BaCO_3$ can be prevented.

An H_2O/CH_4 -ratio of 1.0 is sufficient to suppress the coke formation. The CO-selectivity can also be increased by increasing the feed flow rate. The consequence of increasing the feed flow rate is a decrease in the conversion of CH_4 .

Co-feeding methane and steam allows the POM to be run with a coke free Ni-based catalyst. The CO-selectivity is only slightly lower than without steam.

Acknowledgement

The authors thank the German Federal Ministry of Education and Research for the financial support of the project CaMeRa (catalytic membrane reactor) under the auspices of ConNeCat (competence network catalysis).

References

- [1] J.R. Rostrup-Nielsen, Catal. Today 63 (2000) 159.
- [2] K. Kochloeffl, Steam reforming, in: G. Ertl, H. Knözinger, J. Weitkamp (Eds.), Handbook of Heterogenous Catalysis, vol. 1, VCH-Weinheim, 1997, p. 1819.
- [3] D.A. Hickmann, L.D. Schmidt, Science 259 (1993) 343.
- [4] A. Kleinert, G. Grubert, X.L. Pan, C. Hamel, A. Seidel-Morgenstern, J. Caro, Catal. Today 104 (2005) 267.
- [5] D. Dissanayake, M.P. Rosynek, K.C.C. Kharas, J.H. Lunsford, J. Catal. 132 (1991) 117.
- [6] Y. Teraoka, H.M. Zhang, S. Furukawa, N. Yamazoe, Chem. Lett. 11 (1985) 1743.
- [7] Y. Teraoka, T. Nobunaga, N. Yamazoe, Chem. Lett. 3 (1988) 503.
- [8] Y. Teraoka, T. Nobunaga, K. Okamoto, N. Yamazoe, Solid State Ionics 48 (1991) 207.
- [9] J.E. ten Elshof, H.J.M. Bouwmeester, H. Verweij, Solid State Ionics 81 (1995) 97.
- [10] J.E. ten Elshof, H.J.M. Bouwmeester, H. Verweij, Solid State Ionics 89 (1996) 81.

- [11] L. Qiu, T.H. Lee, L.-M. Liu, Y.L. Yang, A.J. Jacobson, *Solid State Ionics* 76 (1995) 321.
- [12] M. Martin, *J. Chem. Thermodyn.* 35 (2003) 1291.
- [13] U. Balachandran, J.T. Dusek, P.S. Maiya, B. Ma, R.L. Mieville, M.S. Kleefisch, C.A. Udovich, *Catal. Today* 36 (1997) 265.
- [14] U. Balachandran, J.T. Dusek, R.L. Mieville, R.B. Poeppel, M.S. Kleefisch, S. Pei, T.P. Kobylinski, C.A. Udovich, A.C. Bose, *Appl. Catal. A* 133 (1995) 19.
- [15] W. Jin, S. Li, P. Huang, N. Xu, J. Shi, Y.S. Lin, *J. Membr. Sci.* 166 (2000) 13.
- [16] Z. Shao, H. Dong, G. Xiong, Y. Cong, W. Yang, *J. Membr. Sci.* 183 (2001) 18–192.
- [17] C. Tablet, G. Grubert, H. Wang, T. Schiestel, M. Schroeder, B. Langanke, J. Caro, *Catal. Today* 104 (2005) 126.
- [18] J. Caro, H. Wang, C. Tablet, A. Kleinert, A. Feldhoff, T. Schiestel, M. Kilgus, P. Kölsch, S. Peter, *Catal. Today* 118 (2006) 128–135.
- [19] T. Schiestel, M. Kilgus, S. Peter, K.J. Caspary, H. Wang, J. Caro, *J. Membr. Sci.* 258 (2005) 1.
- [20] H. Wang, Y. Cong, W. Yang, *Catal. Today* 104 (2005) 160.
- [21] H. Wang, Y. Cong, W. Yang, *Catal. Today* 82 (2003) 157.
- [22] J. Gillot, B. Lux, P. Cornuault, F. Chaffaut, *Ber. Dtsch. Keram. Ges.* 45 (1968) 224.
- [23] E. Fitzer, B. Kegel, *Carbon* 6 (1968) 433.
- [24] W. Weisweiler, V. Mahadevan, *High Temp. High Pressures* 3 (1971) 111.
- [25] A. Oya, H. Marsh, *J. Mater. Sci.* 17 (1982) 309.
- [26] J. Biscoe, B.E. Warren, *J. Appl. Phys.* 13 (1942) 364.
- [27] K. Hou, R. Hughes, *Chem. Eng. J.* 82 (2001) 311.